SUPPLEMENTAL MATERIAL

to the paper

Self-consistent potential correction for charged periodic systems

Mauricio Chagas da Silva,[1,2,3,†] Michael Lorke,[1] Bálint Aradi,[1] Meisam Farzalipour Tabriz,[1,4] Thomas Frauenheim,[1,5] Angel Rubio,[2,6] Dario Rocca,[3,†] and Peter Deák[1,†]

[1] Bremen Center for Computational Materials Science, University of Bremen, P.O. Box 330440, D-28334 Bremen, Germany.

[2] Max Planck Institute for the Structure and Dynamics of Matter; Luruper Chaussee 149, Geb. 99 (CFEL), 22761 Hamburg, Germany.

[3] Université de Lorraine, CNRS, LPCT, F-54000 Nancy, France.

[4] Max Planck Computing and Data Facility, Gießenbachstr. 2, D-85748 Garching, Germany

[5]Computational Science Research Center, No.10 East Xibeiwang Road, Beijing 100193 and Computational Science and Applied Research Institute Shenzhen, China.

[6] Nano-Bio Spectroscopy Group, Departamento de Fisica de Materiales, Universidad del País Vasco UPV/EHU- 20018 San Sebastián, Spain

Details of the calculations

• *V_C(2-) in bulk diamond:* Simple cubic supercells were considered, with 64, 216, 512, and 1000 atoms, at the experimental lattice constant of 3.56 Å. The unrelaxed defect was created in the middle of the cell. A kinetic energy cutoff of 400 (600) eV was used to expand the wave functions (charge density), and the Γ-point approximation was applied without spin-polarization. For the macroscopic dielectric constant the calculated value of 5.85 was used. The chemical potential of carbon atom was set to the energy per atom in the 2×2×2 supercell (-9.10 eV), as calculated by the same energy setup but with a fine k-mesh of 15x15x15 points. A damping region between (0,0.15) and (0.85,1.0) was added.

• *V_{Cl}(+) on the surface of a NaCl (001) slab:* The supercell had a 3×3 surface unit cell. The starting thickness of the solid part was 3 times the experimental lattice constant (5.64 Å). An unrelaxed vacancy was created on the surface or in the middle of the slab. A kinetic energy cutoff of 262.5 (356.2) eV was used for expanding the wave functions (charge density). Spin-polarized calculations were carried out using the Γ-point approximation. The chemical potential of the Cl atom was set to half the energy of a Cl_2 molecule in a cubic box with lengths of 15 Å, as calculated by the same setup. The value of 2.45 was used in the macroscopic dielectric profile for the solid region.

• *N_CV_C(-) defect in a H-saturated (001) diamond slab:* The solid part consisted of four double-layers with a lateral size of 2√2×2√2, using the experimental lattice constants. Both surfaces were saturated by hydrogen atoms symmetrically, and the minimal thickness of the vacuum part was 15 Å. The ionic positions of the hydrogen atoms, and the carbons attached to them, were fully relaxed first, while keeping the lattice vectors and the rest of a pristine slab fixed at the bulk equilibrium. Then the N_CV_C(-) defect was placed in the middle of the slab (without relaxation). A kinetic energy cutoff of 450 (900) eV was used for expanding the wave functions (charge density). A 2x2x1 Monkhorst-Pack k-point set was used with spin-polarization. For the macroscopic dielectric constant the calculated value of 5.85 was used. A damping region between (0,0.15) and (0.85,1.0) was added in the lateral directions.

• *O_2^- molecule on an anatase-TiO_2 (101) slab:* The solid part consisted of three double-layers with a lateral size of 1×3, using the experimental lattice constants. The thickness of the vacuum layer was 40 Å. The ionic positions were fully optimized. A kinetic energy cut-off of 420 eV (840) eV was applied to expand the wave functions (charge density). Spin-polarized

calculations were carried out using the Γ-point approximation. For the macroscopic dielectric constant the averaged value of 6.68 was used, as calculated in bulk anatase with the same energy setup but with the k-mesh of 6x6x4 points.

A VASP input for all calculations is provided at https://github.com/isobestico/SCPC-Method.

Technical Information

Damping region at the boundary: V_{iso} approaches the edges of the supercell with non-zero derivative (see Fig.S1).

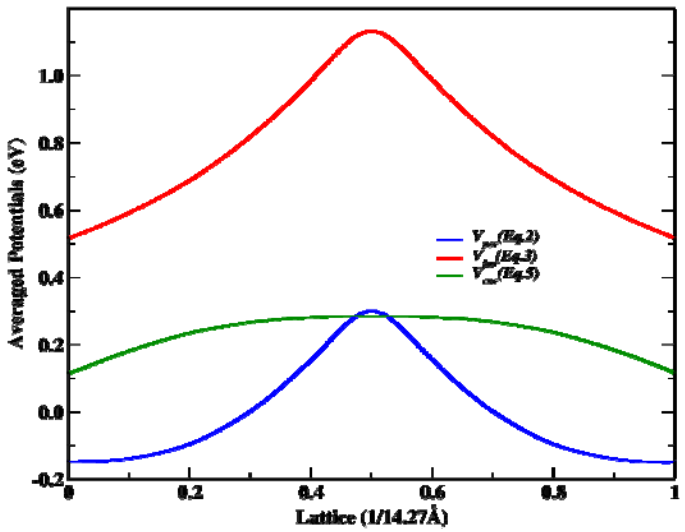

Fig.S1. The periodic (V_{per}(Eq.2)), isolated (V_{iso}(Eq.3)) and corrective (V_{cor}(Eq.5)) averaged potentials, in the lattice direction, of the V_C(2-) in diamond.

Since, because of that, the corrective potential has a cusp at the supercell boundaries, a small charge accumulation occurs there (especially in covalent systems) which, in some cases can cause numerical fluctuations in the total energy. That in turn slows down the convergence of the SCF procedure. For damping these fluctuations and to stabilize the convergence process, a "damping region" in the vicinity of the cell boundary is used in the SCPC method. In this region 10% of the charge distribution of a given iteration step is mixed with 90% of the previous step. To demonstrate the effect of the cusp and of the damping, Fig.S2 shows the variation of the planar average of the charge along the surface normal, and Table.S1 shows the formation energy for the V_C(2-) defect in bulk diamond, with and without application of the damping.

Table S1: The effect of the damping region on the formation energy of $V_C(2-)$ in bulk diamond for different cell sizes. (FNV and SCPC-2 use the pristine system as reference, SLABCC and SCPC-1 the neutral defect.)

Lat. size (Å)	FNV	SCPC-2			SLABCC	SCPC-1		
		Damp.	No Damp	Δ		Damp.	No Damp.	Δ
7.1	12.98	12.89	13.24	0.35	-	12.13	12.08	-0.04
10.7	13.21	13.13	13.35	0.22	13.11	12.87	12.86	0.00
14.3	13.19	13.13	13.29	0.16	13.19	13.01	13.01	0.00
17.9	13.18	13.13	13.24	0.11	13.17	13.05	13.05	0.00

As can be seen in Table.S1, convergence is harder to achieve without the damping, but the final result does not differ much. Users of SCPC are advised to perform a similar check to see if the damping region is required.

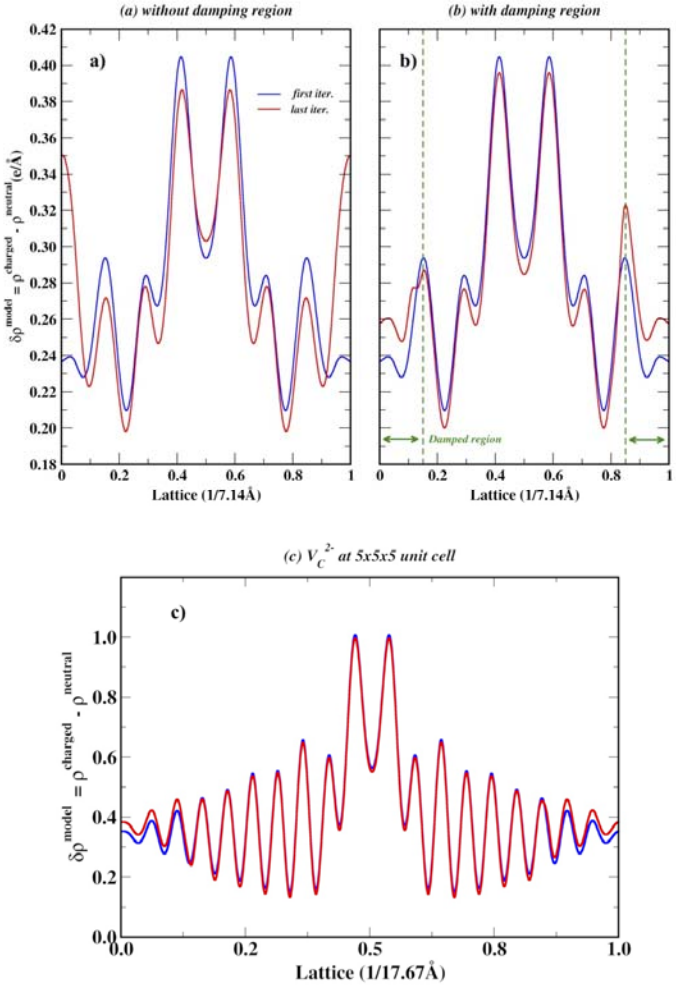

Fig.S2. Planar average of the charge along the surface normal, with (a) and without (b) using a damping region, in case of the $V_C(2-)$ defect in diamond, at the first and last SCF cycle. In (c) the same defect in a large supercell is shown.

Finally we note that, since the screening charge decreases with the distance from the defect, for large supercells this is not an issue, and the correction converges fast, as shown in Fig.S2.c.

Dielectric function in slabs: Fig.S3 shows a typical dielectric profile used in slab calculations. Its form,

$$\varepsilon\left(Z, Z_{low}, Z_{high}, \beta\right)^{-1} = 1 + \frac{1}{4}\left[1 - \epsilon_{mat}^{-1}(z)\right]\left[1 + erf\left(\frac{z - z_{low}}{\beta}\right)\right]\left[1 + erf\left(\frac{z_{high} - z}{\beta}\right)\right]$$

is determined by the parameters Z_{low} and Z_{high}, describing the position of the lower and upper interface, respectively, along the surface normal (Z). These are set by adding the Van-der-Waals radius to the position of the lattice atoms at the boundary. $\epsilon_{mat}$is the (average) dielectric constant of the material, and β is a tunable broadening parameter, with the default value of 0.1 Å, which is appropriate for interfaces of covalent and ionic materials with vacuum. For metal/covalent interfaces a somewhat larger value is needed.

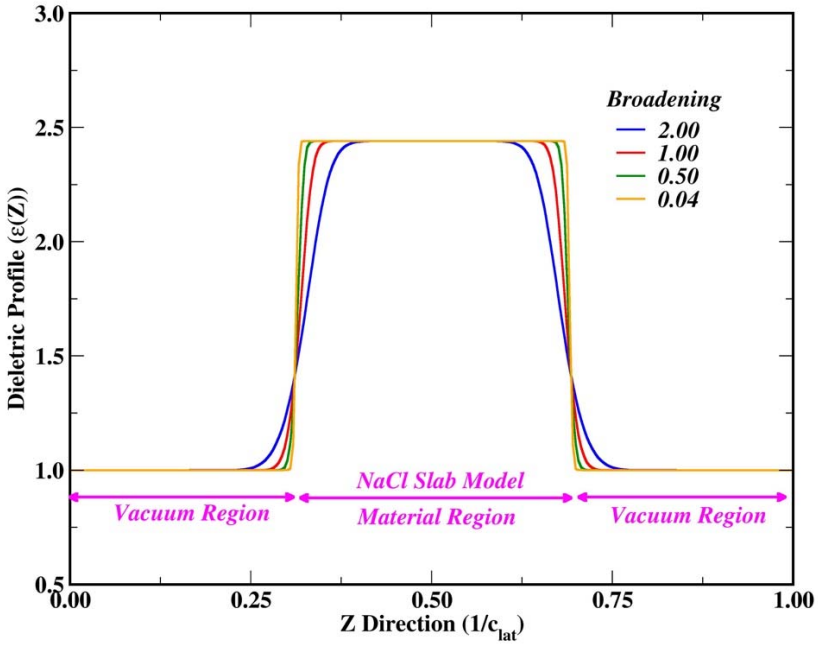

Figure S3: The effect of the broadening factor (β) on the shape of the dielectric function of the NaCl slab.

Convergence Tests

V_C(2-) in bulk diamond: The convergence of the formation energy, and the position of the gap state with the size of the supercell is shown in Fig.S4 and Fig.S5, respectively.

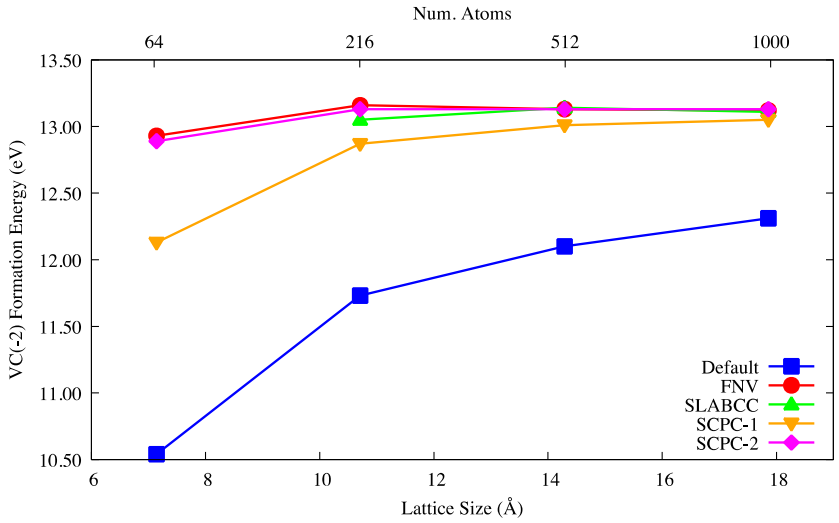

Figure S4. Convergence of the formation energy of the unrelaxed V_C(2-) defect in diamond with lattice (supercell) size. The reference system for SLABCC and SCPC-1 is the neutral defect, for FNV and SCPC-2 the pristine system.

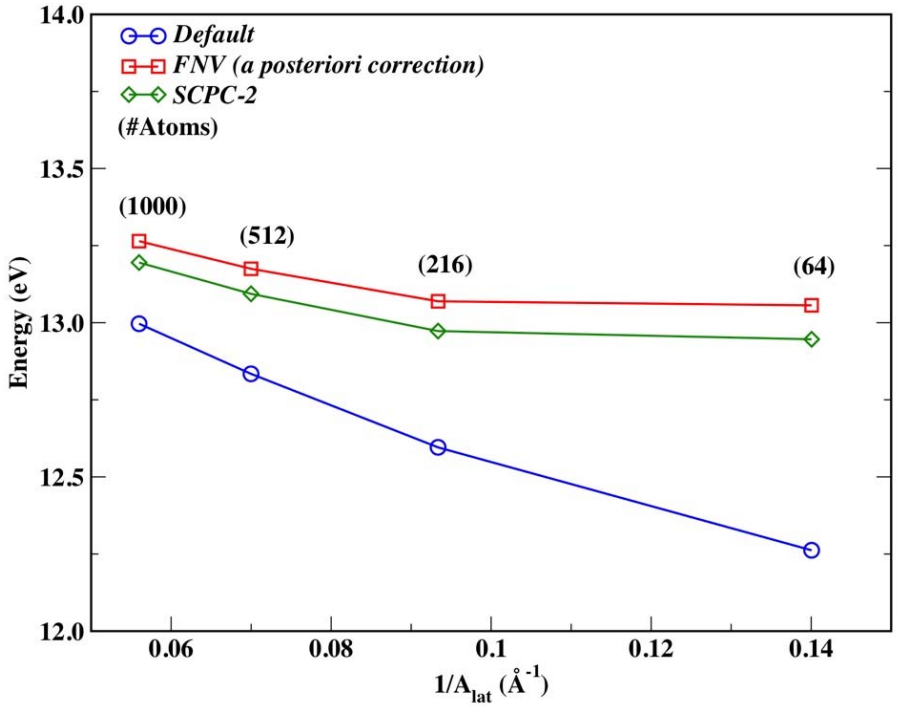

Fig.S5. Comparison of the energy of the triply degenerate gap level of the unrelaxed $V_C(2-)$ in diamond, without (blue curve) and with SCPC-2 (green) to that obtained by using the Chen-Pasquarello formula, with the total energy correction provided by the FNV method (red).

$N_CV_C(-)$ center in bulk diamond.

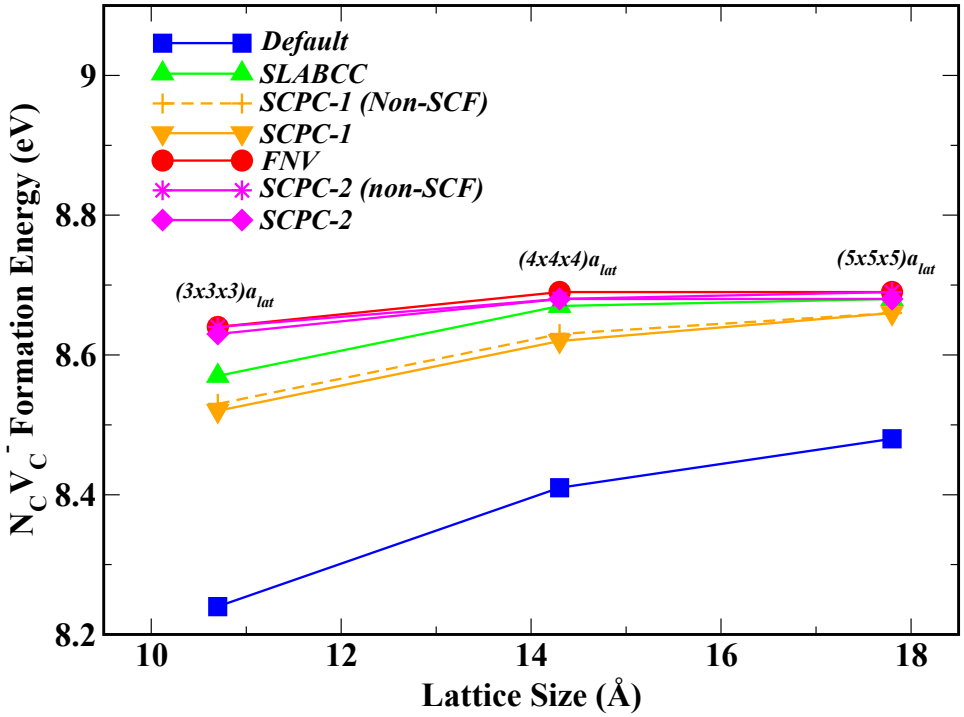

Fig.S6: Convergence of the formation energy of the $N_CV_C(-)$ center in diamond with lattice (supercell) size.

Table.S2: Convergence of the formation energy of the $N_CV_C(-)$ center in diamond with lattice (supercell) size.

Size (Å)	FNV	SCPC-2		SLABCC	SCPC-1	
		Non-SC	SCPC-2		Non-SC	SC
10.7	8.64	8.64	8.63	8.57	8.53	8.52
14.3	8.69	8.68	8.68	8.67	8.63	8.62
17.8	8.69	8.69	8.68	8.68	8.66	8.66

V_{Cl}(+) in bulk NaCl:

Table.S3: Formation energy of V_{Cl}^{+} in bulk NaCl as a function of lattice (supercell) size, calculated with *a posteriori corrections* (FN, SLABCC) and with SCPC. All energy values in eV.

Size (Å)	FNV	SCPC-2		SLABCC	SCPC-1	
		Non-SC	SC		Non-SC	SC
11.3	1.53	1.51	1.45	1.67	1.58	1.51
16.9	1.52	1.50	1.43	1.55	1.52	1.44
22.6	1.51	1.50	1.44	1.53	1.50	1.44
28.2	1.51	1.50	1.43	1.51	1.50	1.43

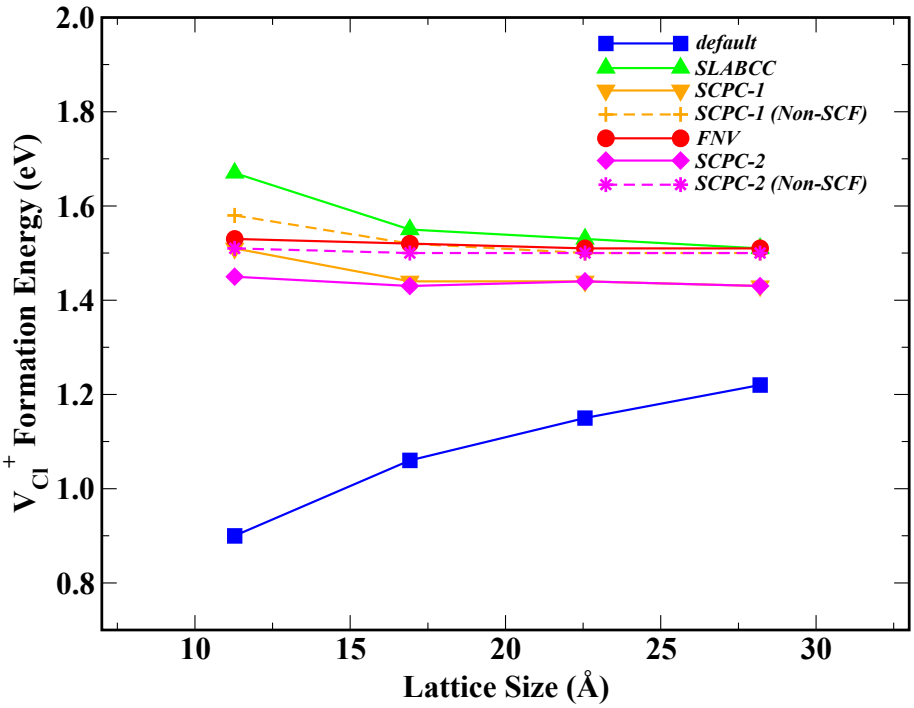

Fig.S7: Formation energy for the V_{Cl}(+) defect in bulk NaCl as a function of lattice (supercell) size.

V_{Cl}(+)on the surface of a NaCl (001) slab:

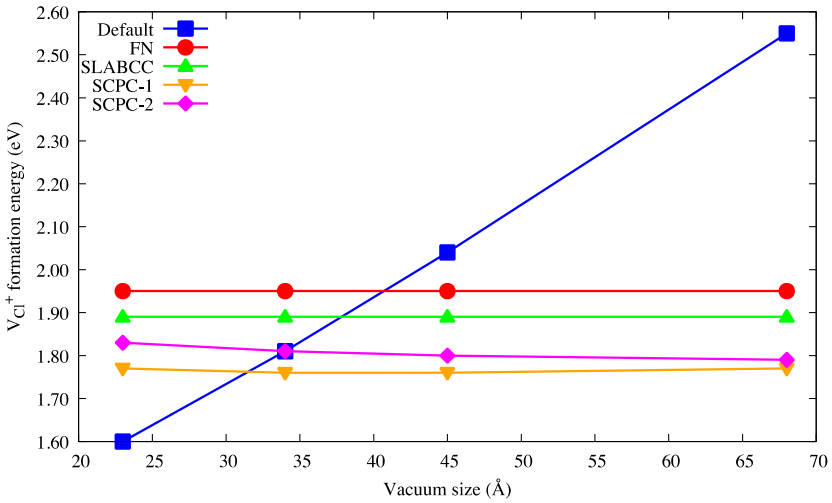

Fig.S8. Convergence of the formation energy of the unrelaxed V_{Cl}(+) on the surface of a NaCl (001) slab with vacuum thickness.

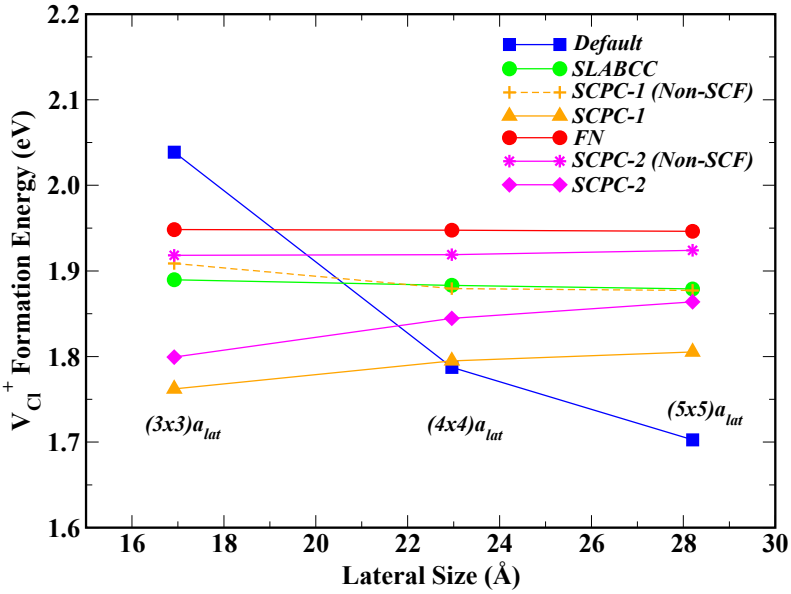

Fig.S9: Convergence of the formation energy of the unrelaxed V_{Cl}(+) on the surface of a NaCl (001) slab (slab thickness of 16.9 Å and vacuum thickness of 45 Å) with lateral size of the slab.

Table.S4: Formation energy of V_{Cl}^{+} on the surface of NaCl (001) slab model (slab thickness 16.9 Å, vacuum thickness 45 Å) with the lateral size of the slab. All energy values in eV.

Lat. Size (Å)	FN	SCPC-2		SLABCC	SCPC-1	
		Non-SC	SC		Non-SC	SC
16.9	1.95	1.92	1.80	1.89	1.91	1.76

23.0	1.95	1.92	1.84	1.88	1.88	1.79
28.2	1.95	1.92	1.86	1.88	1.88	1.81

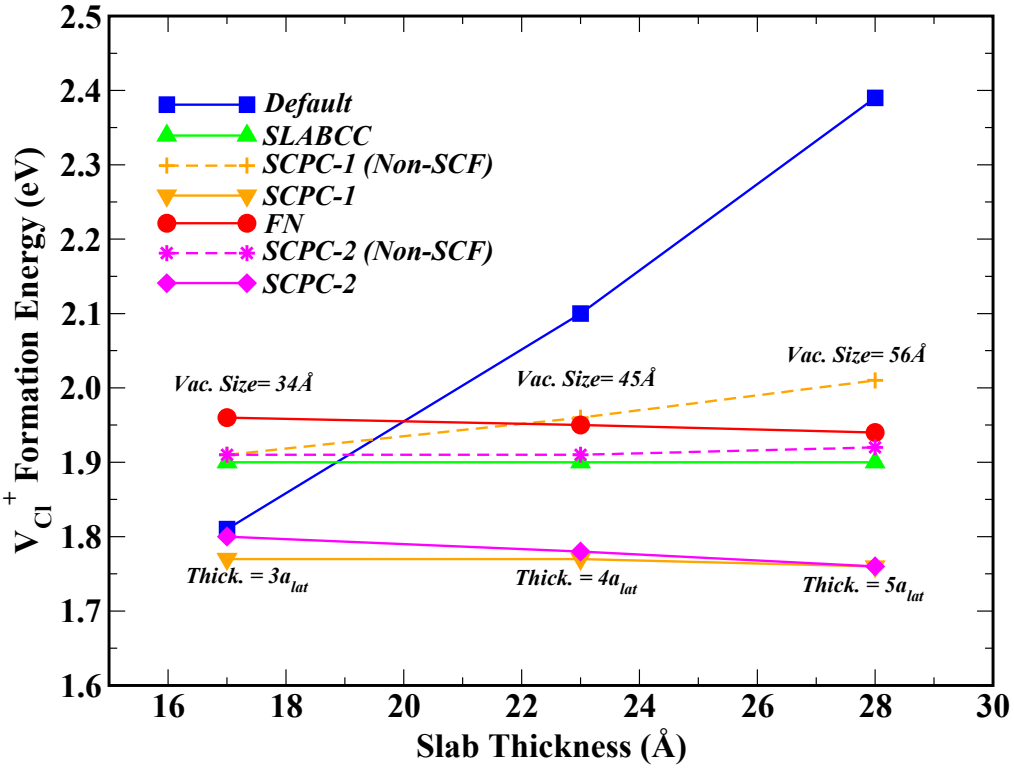

Fig.S10: Convergence of the formation energy of the unrelaxed $V_{Cl}(+)$ on the surface of a NaCl (001) slab (lateral size 16.9 Å) with increasing thickness of the solid part. The ratio between the thickness of the solid and the vacuum part was kept fixed.

Table.S5: Convergence of the formation energy of the unrelaxed $V_{Cl}(+)$ on the surface of a NaCl (001) slab (lateral size 16.9 Å) with increasing thickness of the solid part. The ratio between the thickness of the solid and the vacuum part was kept fixed. All energy values in eV.

Thickness (Å)		FN	SCPC-2		SLABCC	SCPC-1	
Solid	Vacuum		Non-SC	SC		Non-SC	SC
17	**34**	1.96	1.91	1.80	1.90	1.91	1.77
23	**45**	1.95	1.91	1.78	1.90	1.96	1.77
28	**56**	1.94	1.92	1.76	1.90	2.01	1.76

V_{Cl}(+)at the center of a NaCl (001) slab

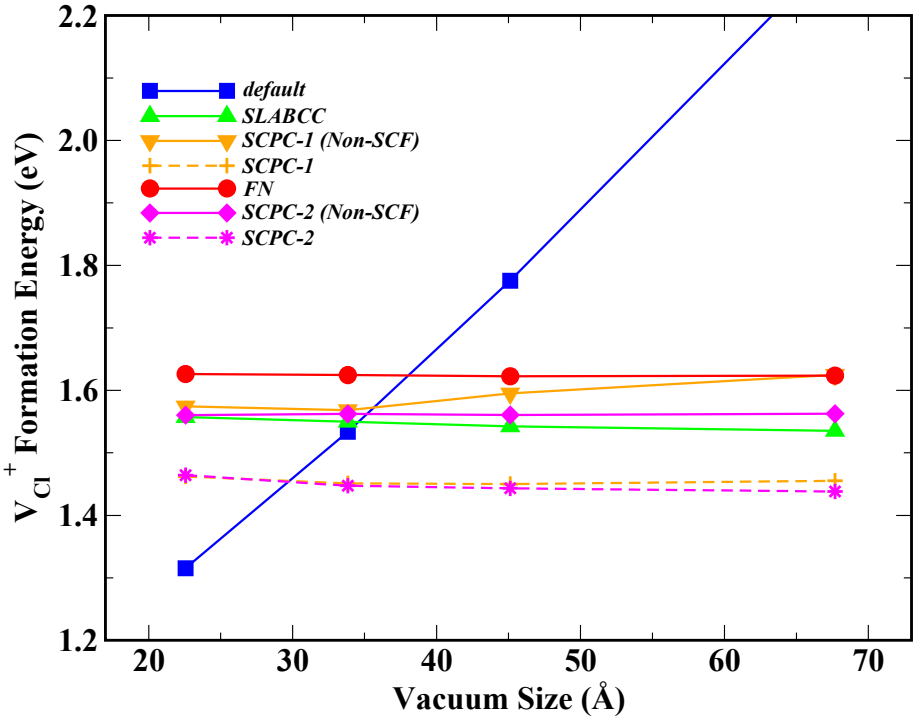

Fig.S11: Convergence of the formation energy of the unrelaxed V_{Cl}(+) in the middle of a NaCl (001) slab with vacuum thickness.

Table.S6: Convergence of the formation energy of the unrelaxed V_{Cl}(+) in the middle of a NaCl (001) slab with vacuum thickness. All energy values in eV.

Vac. Size (Å)	FN	SCPC-2		SLABCC	SCPC-1	
		Non-SC	SC		Non-SCF	SC
22.6	1.63	1.56	1.46	1.56	1.57	1.46
33.8	1.62	1.56	1.45	1.55	1.57	1.45
45.1	1.62	1.56	1.44	1.54	1.60	1.45
67.7	1.62	1.56	1.44	1.54	1.62	1.46

$N_CV_C^-$ center in the middle of a hydrogen saturated diamond (100) slab

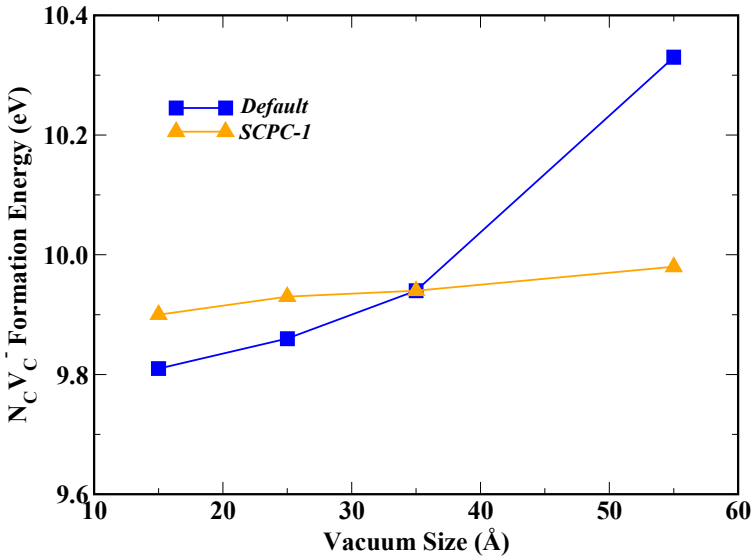

Figure S12: Convergence of the formation energy for the $N_CV_C^-$ center in the middle of a hydrogen saturated diamond (100) slab with vacuum thickness.

Ghost states

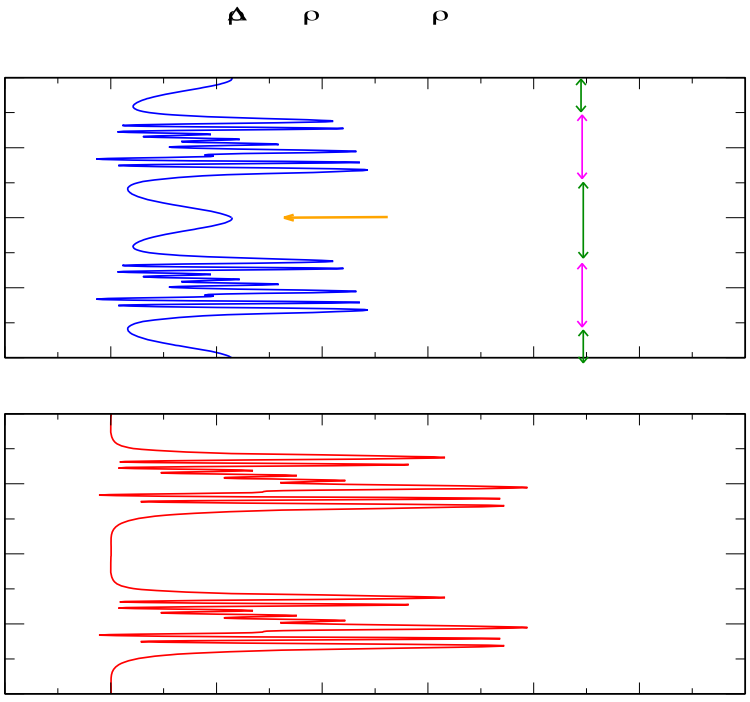

Fig.S13. Planar average of the additional charge along the surface normal for the N_CV_C center in a hydrogen saturated diamond (001) slab without (a) and with (b) SCPC correction. The orange arrow indicates the middle of the vacuum region.

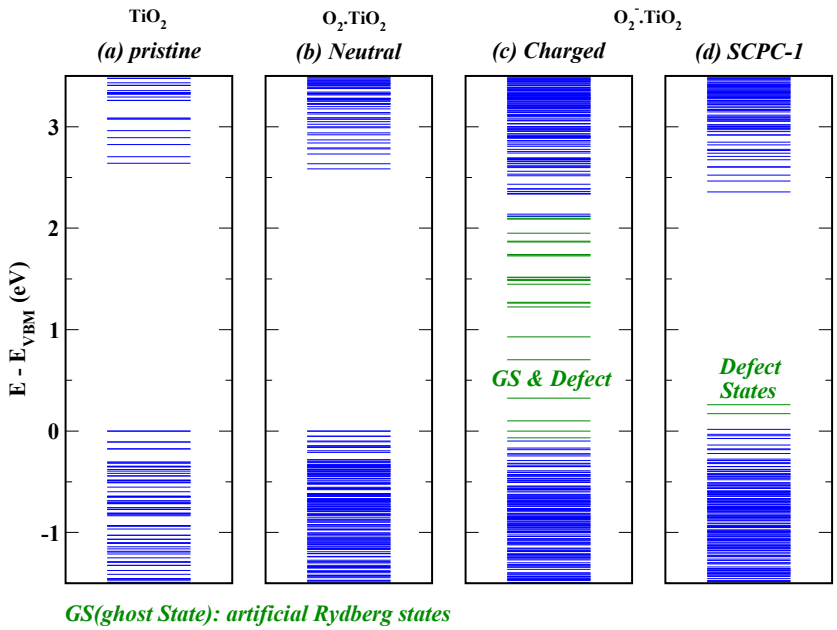

Fig.S14. One-electron states of an anatase-TiO_2 (101) slab without (a) and with an adsorbed O_2 molecule on the surface: neutral case (b), negatively charged case without (c) and with SCPC (d).

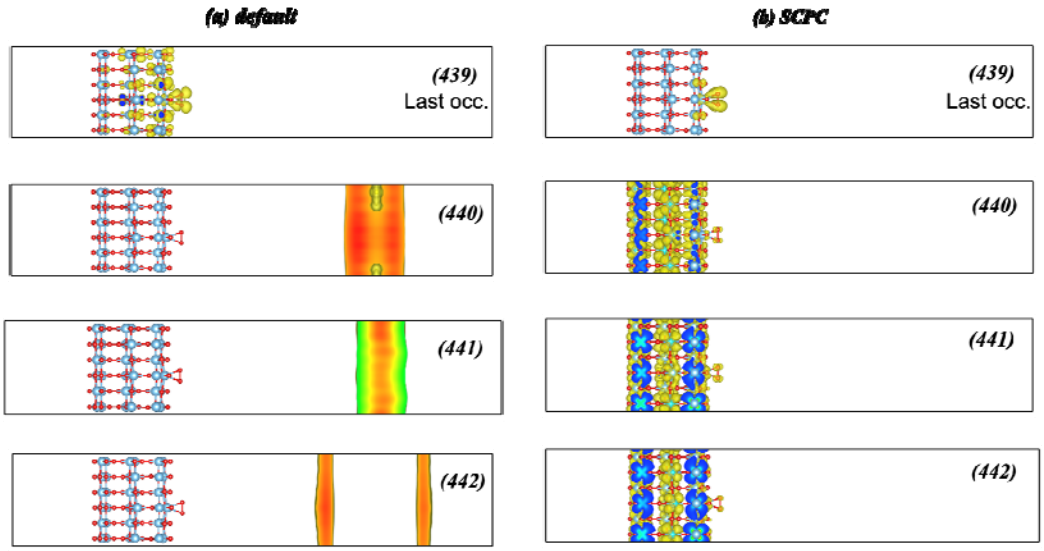

Fig.S15. Square of the wavefunction without (default) and with SCPC for four selected states which are in the gap of Fig.S6.c, an isosurface value of 0.0002 e/Å^3 was used for plotting.